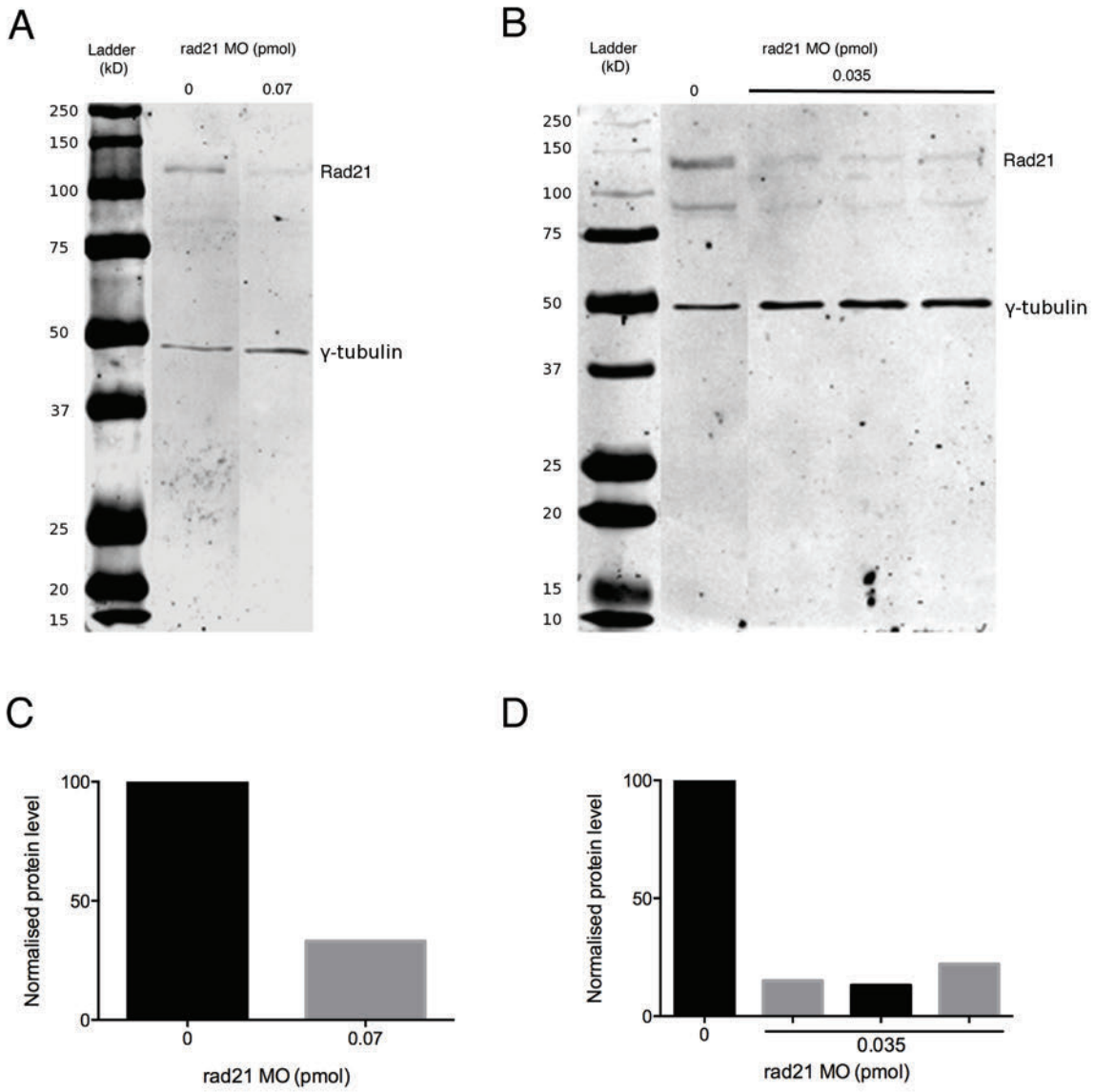

Figure S1. Low doses of Rad21 morpholino (MO) decrease but do not entirely abolish Rad21 protein. Rad21 protein quantity was analysed by Western blot in mock-injected and Rad21 MO-injected embryos from two independent experiments. Protein was extracted from 12-somite stage embryo lysates. (A) Western blot of Rad21 protein level in embryos injected with 0 and 0.07 pmol Rad21 morpholino. (B) Western blot of Rad21 protein level in embryos injected with 0 and 0.035 pmol Rad21 MO (biological triplicates were loaded). In (A) and (B), γ-tubulin protein was detected as a loading control. (C-D) Graphs show quantification of Rad21 protein level in the blots above, normalized to the 0 pmol controls. Rad21 protein levels were reduced 70-80% following morpholino injection.

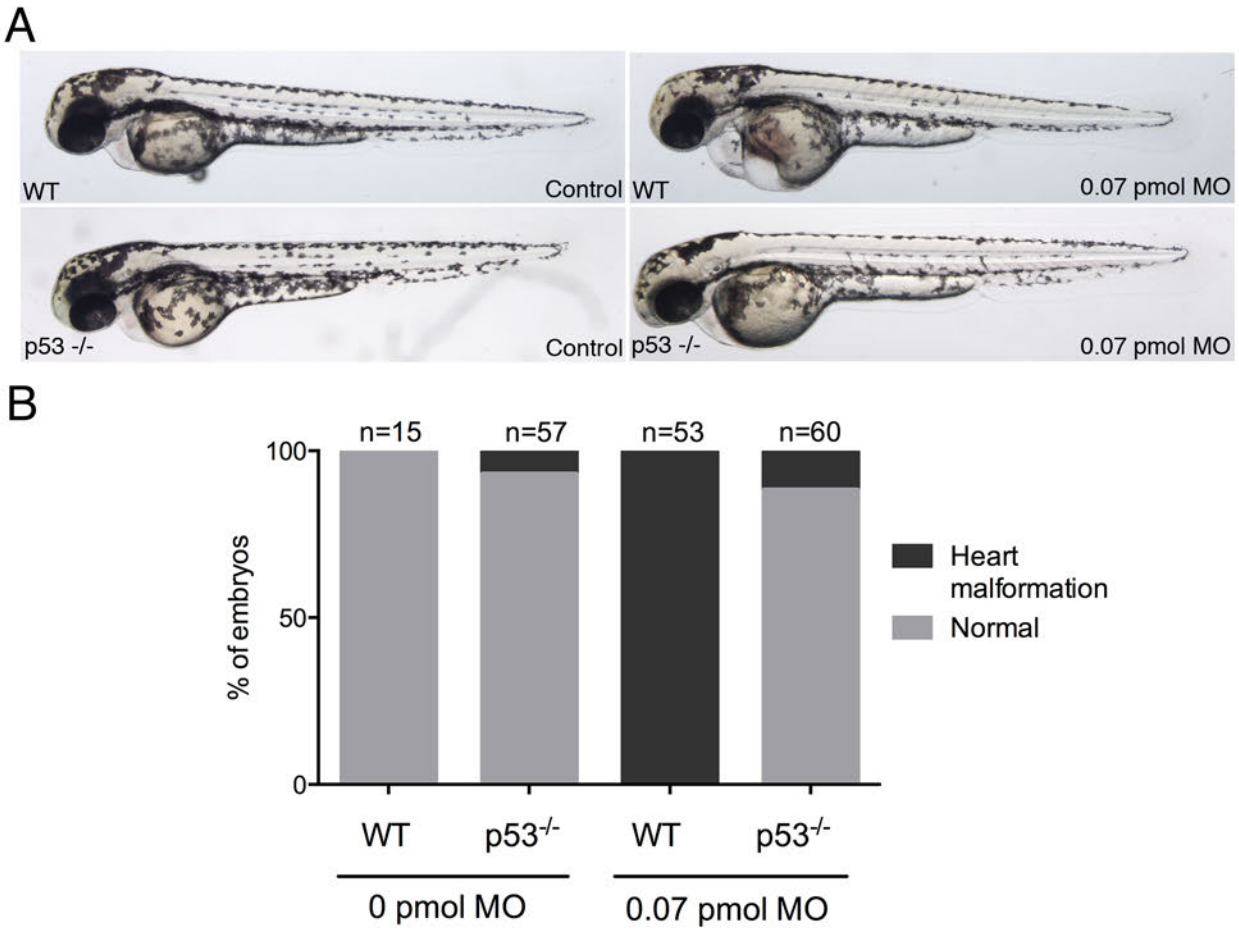

Figure S2. p53 deficiency rescues heart malformations caused by Rad21 depletion. Wild-type (WT) and p53 homozygous mutant ($p53^{zdf1}$) embryos were injected with 1 nl 0.07 pmol Rad21 ATG MO, or 1 nl phenol red dye solution (0 pmol controls) at the 1-cell stage. (A) Embryos were examined at 2 days post fertilization (2 dpf). Embryos shown are representative examples of 2 dpf phenotypes, lateral views with anterior to the left. (B) Rad21 MO caused heart malformations in 53/53 of WT embryos, while 53/60 $p53^{zdf1}$ homozygous embryos had normal hearts fol lowing injection with Rad21 MO. Graph shows percentage of embryos with each phenotype at 2 dpf. Total number of embryos per group is shown above bars.

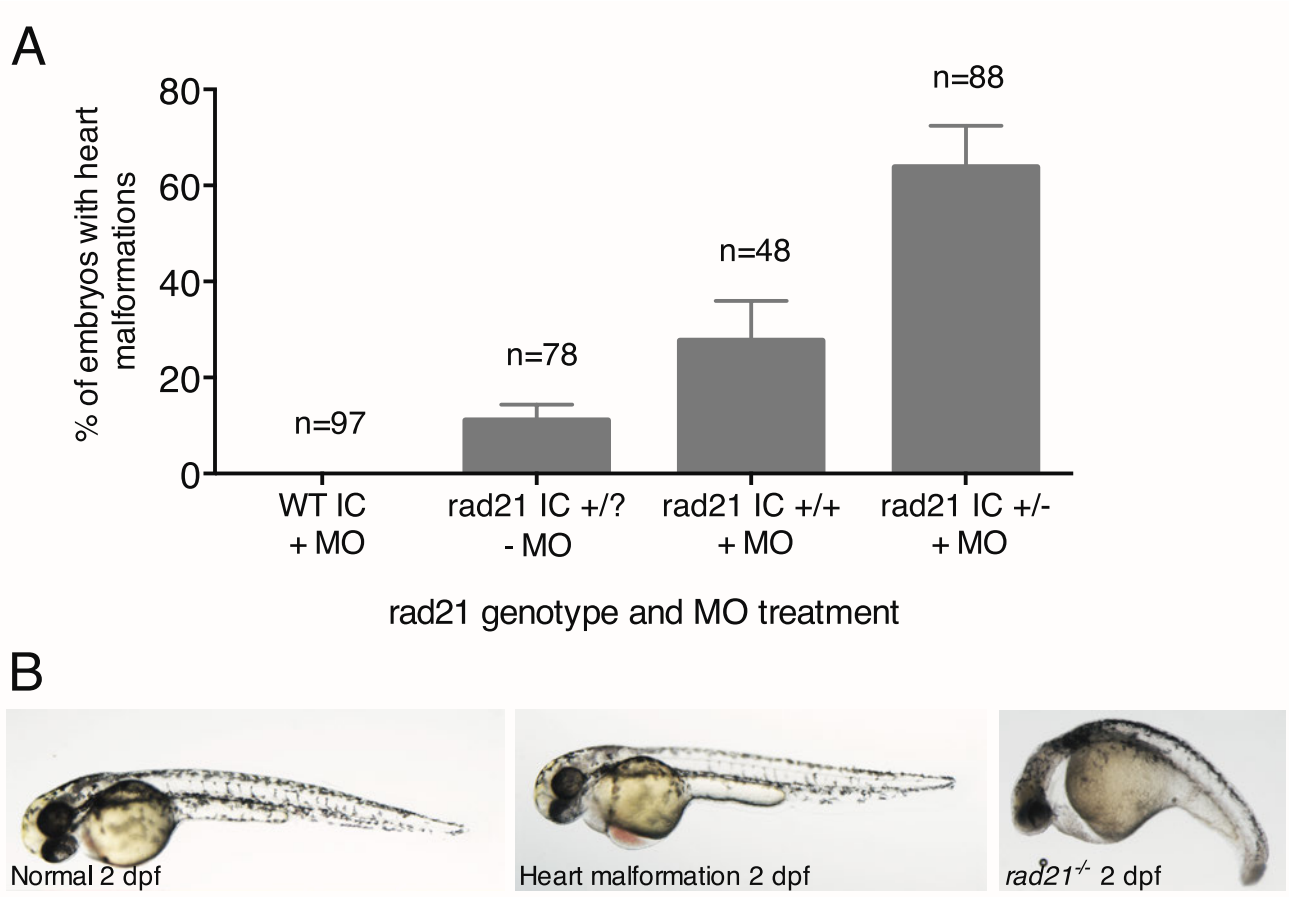

Figure S3. The Rad21 morpholino (MO) causes heart defects specifically through the *rad21* genetic pathway. Embryos from wild-type incrosses (WT IC) and *rad21*$^{nz171/+}$ incrosses (rad21 IC) were injected with 0.02 pmol Rad21 MO (+ MO). At this dose, we never observed heart defects in embryos from a WT IC background, indicating that this dose of morpholino has no effect on a wild type background. However, the same dose caused heart defects in embryos from a *rad21*$^{nz171/+}$ IC background, indicating that the MO interacts specifically with the *rad21* genetic pathway. (A) Graph showing percentage of embryos with heart malformations in each treatment group. +/? refers to *rad21*$^{nz171/+}$ IC embryos in which it is unknown if the genotype is wild type (+/+) or heterozygous (+/-). Data are means of 3 independent biological replicates. Total numbers of embryos per group are displayed above the bars. Error bars are ± SEM. The level of Rad21 was significantly associated with frequency of heart defects, χ^2 (3, N=311), 109.4, $p<0.0001$). (B) Example images showing how embryos were classified based on phenotype at 2 days post-fertilisation (dpf). Views are lateral with anterior to the left. *rad21* null mutants were excluded from this assay, and were identified on the basis of the characteristic phenotype shown (far right).

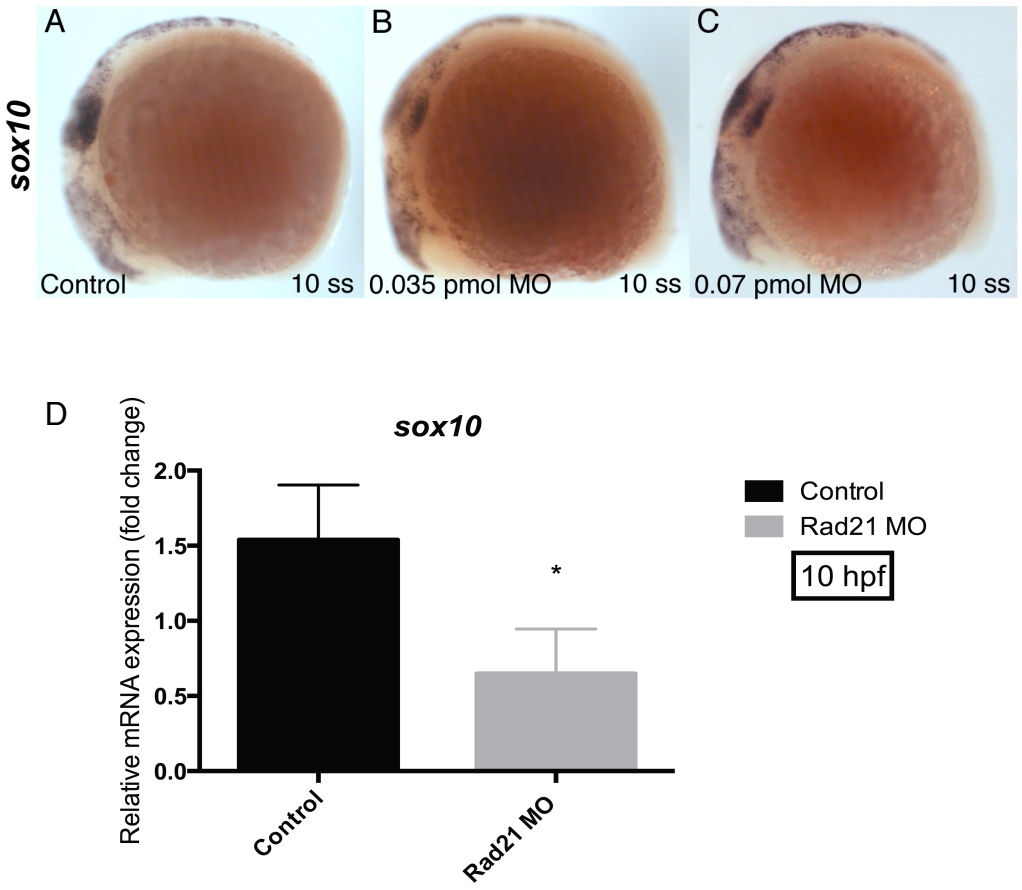

Figure S4. Minor Rad21 depletion does not prevent neural crest cell specification or early migration as judged by spatial *sox10* expression, but modest depletion does reduce the quantity of *sox10* mRNA. Zebrafish embryos were injected at the 1-cell stage with 1 nl phenol red dye (controls), or with 0.035 pmol or 0.07 pmol Rad21 ATG MO. The expression pattern of the neural crest (NC) marker gene *sox10* was examined by in situ hybridisation at the 10-somite stage (10 ss). Images were taken of whole mount embryos, lateral view with anterior to the left. (A) Control embryo. In controls, *sox10* expression marks NC cells at their site of specification along the neural tube, as well as early migration of NC cells to the anterior (n=24). (B-C) Rad21-depleted embryos. In embryos depleted of Rad21 using either 0.035 pmol (B) or 0.07 pmol (C) morpholino, the *sox10* expression pattern was no different to controls (0.035 pmol, MO n =18, 0.07 pmol, MO n = 9). (D) Quantitative RT-PCR analysis of *sox10* mRNA expression in 10 hpf embryos, comparing control and Rad21 MO-injected embryos (0.5 pmol MO). The Y axis indicates relative mRNA levels, normalised to *rpl13a* and *actb* mRNA. Data were generated from the same samples used for RNA-seq (Table S1), and represent the mean of three independent biological replicates. Error bars are standard error of the mean. Asterisk indicates a significant change in *sox10* expression (p <0.05).

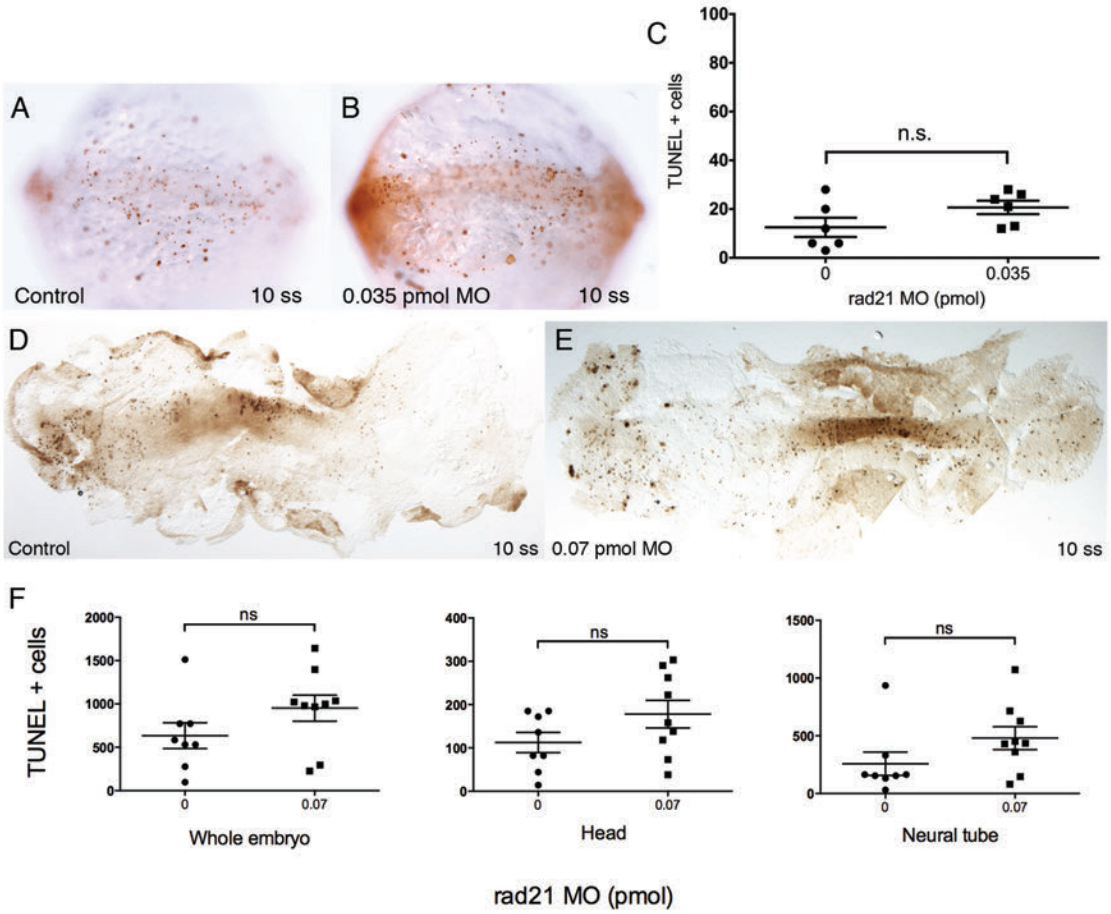

Figure S5. Rad21 depletion caused a slight, non-significant increase in cell death. Zebrafish embryos were injected at the 1-cell stage with 1 nl phenol red dye (controls), or with 0.035 or 0.07 pmol Rad21 ATG MO as indicated. Apoptosis was examined by TUNEL staining once injected embryos had reached the 10-somite stage. (A, B) Representative images of control (n=6) and Rad21-depleted (n=6) whole-mount, TUNEL-stained embryos, dorsal views, anterior to the left. (C) Graphs show the mean number of TUNEL-stained cells along the axis of whole-mount 0.035 pmol MO-injected and control embryos. (D, E) Representative images of control (n=8) and Rad21-depleted (n=9) embryos. Images are of flat mounted embryos, dorsal view, anterior to the left. (F) Graphs show the mean number of TUNEL-stained cells in whole embryos (left) and the neural crest cell-containing head (centre) and neural tube (right) regions. Each data point represents an individual embryo. Apoptosis was not significantly increased by Rad21-depletion (p>0.05, unpaired t-test). Error bars are ±SEM. The 0.07 pmol Rad21 MO dose elicited a trend toward increased apoptosis.